Article

Experimental Investigation on CIRCE-HERO for the EU DEMO PbLi/Water Heat Exchanger Development

Pierdomenico Lorusso [1], **Emanuela Martelli** [2], **Alessandro Del Nevo** [1,*], **Vincenzo Narcisi** [3], **Fabio Giannetti** [3] and **Mariano Tarantino** [1]

1   ENEA FSN-ING-SIS—Department of Fusion and Nuclear Safety Technology, Experimental Engineering Division, Systems and Components Design Laboratory, C.R. Brasimone, 40032 Camugnano, Italy; pierdomenico.lorusso@enea.it (P.L.); mariano.tarantino@enea.it (M.T.)
2   ENEA FSN-FUSTEC-TES—Department of Fusion and Nuclear Safety Technology, Fusion Technology Division, Nuclear Technology Laboratory, C.R. Frascati, I-00044 Frascati, Italy; emanuela.martelli@enea.it
3   Sapienza University of Rome, Department of Astronautical, Electrical and Energy Engineering (DIAEE), 00186 Rome, Italy; vincenzo.narcisi@uniroma1.it (V.N.); fabio.giannetti@uniroma1.it (F.G.)
*   Correspondence: alessandro.delnevo@enea.it; Tel.: +39-0534-801-130

Abstract: The present paper describes the experimental campaign executed at the ENEA Brasimone Research Centre aiming at supporting the development of a PbLi/water heat exchanger suitable for the lithium–lead loops of the dual coolant lithium lead and the water cooled lithium lead breeding blankets of the EU DEMO fusion reactor. The experiments were performed in a test section named HERO, installed inside the main vessel of the lead–bismuth eutectic-cooled pool-type facility CIRCE. The test section hosts a steam generator bayonet tube mock-up in relevant scale, which was selected as a promising configuration for DEMO purposes. For the thermal-hydraulic characterization of the component, five tests were executed at different water pressures (6, 8, 12 MPa, two tests at 10 MPa), and liquid metal flow rates (40, 33, 27, 20, 10 kg/s). The experimental outcomes proved the technological feasibility of this novel steam generator and its suitability for the DEMO PbLi loops. The activity was completed with a post-test analysis using two versions of the system code RELAP5. Because the experiments were executed with lead–bismuth eutectic, a scaling analysis is proposed to find the equivalence with PbLi. RELAP5 code was applied to recalculate the experimental data using PbLi as working fluid.

Keywords: EU DEMO fusion reactor; heavy liquid metal technology; steam generator bayonet tube

1. Introduction

Within the EUROfusion R&D program, financed by the EU Horzon 2020 programme, for the realization of the demonstration fusion power reactor (DEMO) [1], a study was performed to support the development of a lithium–lead (PbLi)/water heat exchanger (HEX). Such a component is in charge of removing the nuclear heat deposited in the PbLi of the dual coolant lithium lead (DCLL) breeding blanket (BB) [2], producing steam suitable to properly feed the turbine unit, ensuring an efficient conversion of the thermal power to electricity. Moreover, the same design is suitable for removing the power deposited in the PbLi in case of unbalance in the water coolant lithium lead (WCLL) BB [3]. One of the configurations selected for DEMO purposes was the steam generator with bayonet tubes (SGBT) [4]. The SGBT concept stands out for its safety features, i.e., the reduced occurrence of water-Pb/Pb-alloy interaction [5–7], thanks to a double physical separation between the coolants and an easier monitoring of eventual leakages by pressurizing the separation region with inert gas.

The double wall concept has been studied since the 1960s for sodium reactor applications [8], with the aim of increasing the safety margin of the nuclear power plants by reducing the occurrence of liquid metal/water interaction. In fact, the use of Steam Generators (SG) with a single wall implies the possibility of a liquid metal–water reaction in case

of tube rupture, negatively impacting the operation and safety of such plants. Besides the enhanced safety, the use of double wall tubes experienced in experimental breeder reactor (EBR) I and EBR II highlighted that despite the higher initial cost respective to the single wall tubes, the cost in terms of plant life and maintenance are lower [8], making the double wall solution convenient not only for safety concerns but also from an economical point of view.

The double wall concept, improved with the introduction of leakage monitoring abilities and the bayonet tube geometry, has been proposed for Generation IV heavy liquid metal fast reactors [9–11]. In particular, the solution turned out to be interesting for the pool-type lead fast reactors, where the steam generators are directly installed inside the reactor tank, acting as interface between the nuclear island and the secondary system. The adoption of a double wall allows the use of an intermediate loop and an intermediate heat exchanger to be avoided.

Similar considerations about the safety concerns can be applied to the fusion applications involving the use of liquid metals as coolant. For these reasons, the features of the SGBT make it suitable not only as SG for the DCLL BB PbLi loop, but also exploitable as HEX for the WCLL BB PbLi loop.

Since the SGBT solution to be connected to the PbLi system is prototypical, a set of experimental tests were planned and executed at ENEA Brasimone Research Centre (R.C.) to demonstrate the technological feasibility and performances of the component [12–14]. The test section (TS) involved in the experimental campaign was HERO (Heavy Liquid mEtal pRessurized water cOoled tubes) [15], which hosts a relevant scale mock-up of an SGBT consisting of a bundle of seven double-wall bayonet tubes with a dedicated leakage monitoring system. This test section, designed at ENEA Brasimone R.C. and implemented in the main vessel of the lead–bismuth eutectic (LBE)-cooled pool-type facility CIRCE (CIRColazione Eutettico) [16], deals with the investigation of the thermal-hydraulic features of prototypical systems and components, providing at the same time an experimental database suitable for thermal-hydraulic validation of numerical tools (i.e., system codes and Computational Fluid Dynamic codes). The HERO SGBT unit was connected to a dedicated secondary loop that provides the feedwater at high temperature and pressure (up to 18 MPa). Both primary and secondary systems were instrumented for monitoring and control of the facility operation, as well as to acquire a complete set of experimental data.

The thermal-hydraulic characterization of the HERO SGBT was executed through a set of five experimental tests [12] with different water pressures (6 MPa, 8 MPa, two tests at 10 MPa, 12 MPa). In each of the five tests, an experimental sensitivity analysis was carried out, changing the mass flow rate of the LBE in four tests (40, 33, 27, 20, 10 kg/s) and the flow rate of SGBT feedwater in the repeated test at 10 MPa (LBE mass flow rate constant at 27 kg/s). The experimental outcomes were used to demonstrate the technological feasibility of the prototypical SGBT, proving its suitability for the PbLi loops of DCLL BB and WCLL BB.

On the basis of the secondary circuit layout and the HERO SGBT geometry, a numerical post-test analysis was performed using two versions of the RELAP5 code: the RELAP5-3D© Ver. 4.3.4 [17] and a modified version of the RELAP5/Mod3.3 [18,19], which includes heavy liquid metals as working fluids. The numerical outcomes were compared with the experimental results in order to assess the code capability in predicting thermal-hydraulic performances of the component and to study the heat transfer in liquid metal, supporting the code validation process for fusion applications.

Finally, a further analysis was carried out, applying scaling methods to assess a correspondence between the LBE and the PbLi [12]. The scaling was performed in two different ways, i.e., preserving the convective heat transfer (method #1) and preserving both the thermal power and the temperature difference (method #2).

The present paper aims at describing the HERO SGBT main features, along with the primary and secondary systems of the CIRCE facility. Then, the experimental tests are presented along with the experimental outcomes achieved, focusing on the thermal-

hydraulic performances of the HERO SGBT when operated in different working conditions. The computational analysis and the scaling methods for LBE and PbLi are presented to provide a complete thermal-hydraulic analysis of the HERO SGBT.

2. CIRCE-HERO Layout

The pool-type LBE-cooled facility CIRCE is an experimental platform located at ENEA Brasimone R.C. [20,21] and used to perform large-scale integral tests [22] and component thermal-hydraulic characterization [13,23]. The facility consists of a cylindrical main vessel, heating and cooling systems for LBE, storage and transfer tanks, and auxiliary systems for LBE circulation and gas recirculation. The main vessel has a height of about 8500 mm, an inner diameter of 1170 m, and a wall thickness of 15 mm. The vessel stores an LBE amount of about 70 tons (up to 500 mm from the top flange), covered with inert gas (argon) maintained at ~0.2 barg.

The HERO TS is installed within the CIRCE main vessel from the top through a coupling flange. The CIRCE main vessel along with the HERO TS main components are shown in Figure 1. The LBE flows upwards, passing through the heating source called the fuel pin simulator (FPS, red in Figure 1) consisting of 37 electrically heated pins, then it reaches the fitting volume (green) and it flows through the riser (yellow) up to the separator (gold), where the LBE free level reaches about the middle height of the walls. From the separator, the LBE enters the shell side of the SGBT (blue) and it flows downwards, coming back into the pool. The LBE circulation is performed thanks to the difference in height of the thermal barycenters of FPS and SGBT (natural circulation) or by means of an argon injection device, consisting of a nozzle connected to a dedicated argon line and placed at the riser inlet section, which allows it to enhance the LBE circulation (gas-enhanced circulation). The mixture of LBE/argon flows upward through the riser. Then, once that the mixture reaches the separator, the LBE is naturally separated from the argon, which migrates in the cover gas of the main vessel while the pure LBE flows in the shell side of the SG. Thanks to the separator, it is possible to avoid the argon inlet inside the steam generator.

The HERO SGBT is an experimental mock-up that uses heavy liquid metal (i.e., LBE in CIRCE) as the primary working fluid (shell side) and pressurized water as the secondary coolant (tube side). It is designed to study the thermal-hydraulic performances of an SGBT in nuclear applications involving heavy liquid metals as the primary coolant. The component has undergone several experimental campaigns in a broad range of operating conditions, supporting in such a way the development of heavy liquid metal technologies for fission [22,23] and fusion [12,13] applications, as well as the validation process of numerical tools [24–26].

The technical draw of the HERO SGBT unit is depicted in Figure 1. It is composed of:

- The helium chamber (ex-vessel), for pressurizing the AISI316L powder gap with inert gas;
- The steam chamber (ex-vessel), collecting the steam arising from the bayonet tubes (BTs);
- The tube bundle, composed of 7 BTs with an active length of 6000 mm, arranged with a triangular pitch in a hexagonal shroud; and
- The top flange on the top of the main vessel, which sustains the steam and helium chambers, the BTs, and the hexagonal shell.

Each of the seven BTs consists of four coaxial tubes, as depicted in Figure 2: the slave tube, through which the feedwater flows downward; the first and second tube, forming the annular region where the steam is produced flowing upward; and finally, the third tube, which forms with the second tube a gap pressurized with helium at ~0.8 MPa to detect any leakages and is filled by AISI316L powder. The adoption of the stainless-steel powder allows the heat exchange to be increased and, thus, the overall performance of the component, thanks to its good thermal conductivity. The slave and first tube form a first annular gap filled by air acting as an insulator to avoid steam condensation. The hydraulic connection of the SGBT with the LBE circulating in the primary system is obtained by

means of six openings drilled into the SG hexagonal shroud 300 mm above the separator bottom, which allow the primary coolant inlet on the SG shell side.
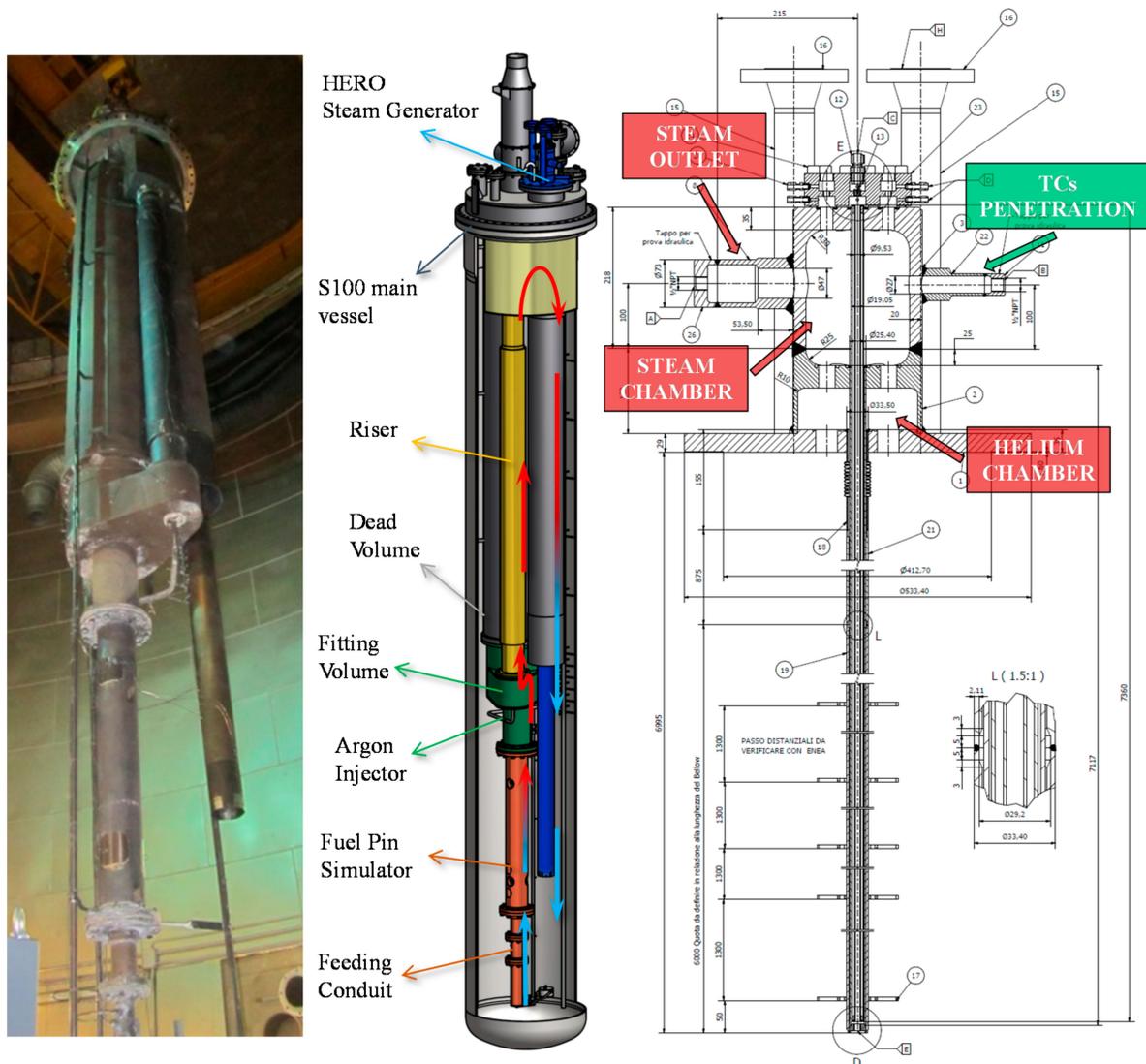
Figure 1. A 3D sketch of CIRCE-HERO and a technical drawing of the HERO SGBT.

A dedicated once-through secondary loop is installed to feed the SGBT with demineralized water at high temperature and pressure (up to 18 MPa). The water loop, depicted in Figure 3, is composed of a feeding line composed of a demineralizer, a volumetric pump, a helical pre-heater, and a manifold for the water distribution among the seven BTs. Downstream of the SGBT, the steam chamber is connected to a discharge line that allows the exit of the steam produced by the SG to the environment. Furthermore, upstream of the manifold, a bypass line is installed and used for the operational transients of the system (i.e., startup and shutdown phases). A helium line is also installed for pressurizing the AISI316L powder gap of the BTs at ~0.8 MPa.

Both the primary and secondary systems are instrumented for monitoring and operating the facility, as well as to acquire experimental data. On the primary system, 119 TCs are distributed along the pool to capture mixing and stratification phenomena [16]. Each component of the TS is equipped with thermocouples located at the inlet and outlet sections (e.g., fitting volume, riser, separator) for their thermal-hydraulic characterization. The FPS and the SGBT shell side is more deeply instrumented by bulk TCs and wall TCs, positioned at the inlet/outlet sections and at different elevations in different sub-channels

for better monitoring of the temperatures along their active lengths. Details on the FPS TC positions can be found in [27], whereas the TCs installed along the LBE side of the SGBT are reported in Figure 3 (red and azure identification codes for bulk and wall temperatures, respectively) in order to facilitate the comprehension of the experimental outcomes. A Venturi flow meter (VFM) is installed upstream of the FPS to measure the LBE mass flow rate. Bubble tubes injecting argon [28] are installed for absolute and differential pressure measurement within the main vessel and along the TS.
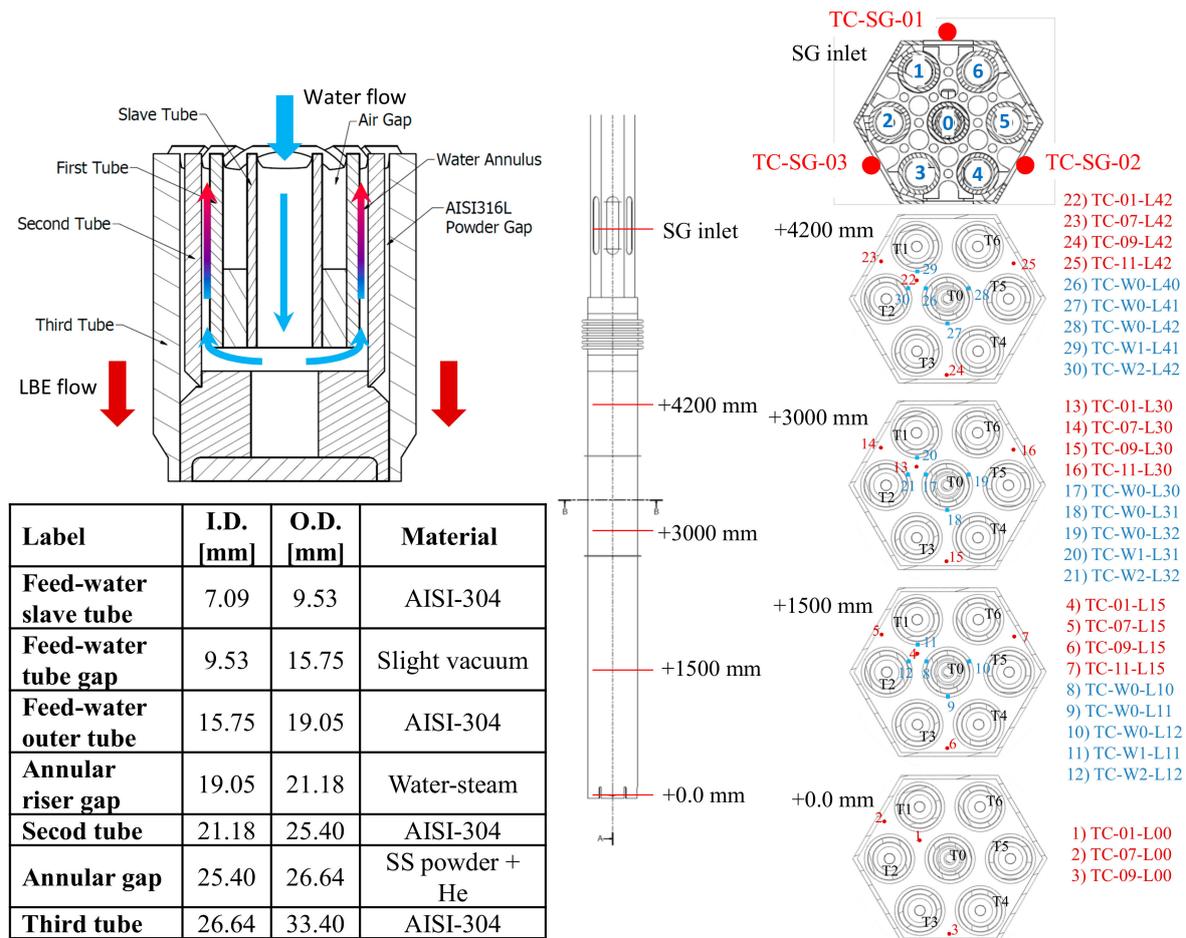

Label	I.D. [mm]	O.D. [mm]	Material
Feed-water slave tube	7.09	9.53	AISI-304
Feed-water tube gap	9.53	15.75	Slight vacuum
Feed-water outer tube	15.75	19.05	AISI-304
Annular riser gap	19.05	21.18	Water-steam
Secod tube	21.18	25.40	AISI-304
Annular gap	25.40	26.64	SS powder + He
Third tube	26.64	33.40	AISI-304

Figure 2. Details of the bayonet tube geometry and SGBT primary side instrumentation.

Figure 3 reports the secondary loop along with the instrumentation installed. The feedwater mass flow rate is measured with a Coriolis flow meter upstream of the pre-heater and seven mini turbine flow meters (TFMs, in azure) are installed on each feeding tube in order to highlight possible unbalanced flow. For the purposes of the paper, it is worth focusing on the SGBT instrumentation. A total of 12 TCs are placed in the annular riser of the bayonet tubes:

- Five TCs located in the central tube, named T0 and set at different levels (+500 mm, +1500 mm, +3000 mm, +4200 mm, +6000 mm, assuming the bottom part of the bayonet tube is 0 mm), aiming to characterize water vaporization;
- Seven TCs at the exit of each bayonet tube annular riser;
- Three TCs at the steam chamber outlet to detect eventual condensation and radial stratification; and
- Four differential pressure transmitters to measure the pressure across 4 BTs in order to characterize pressure drops in single- and two-phases flow conditions.

More details on the CIRCE-HERO instrumentation can be found in [15,16,23].
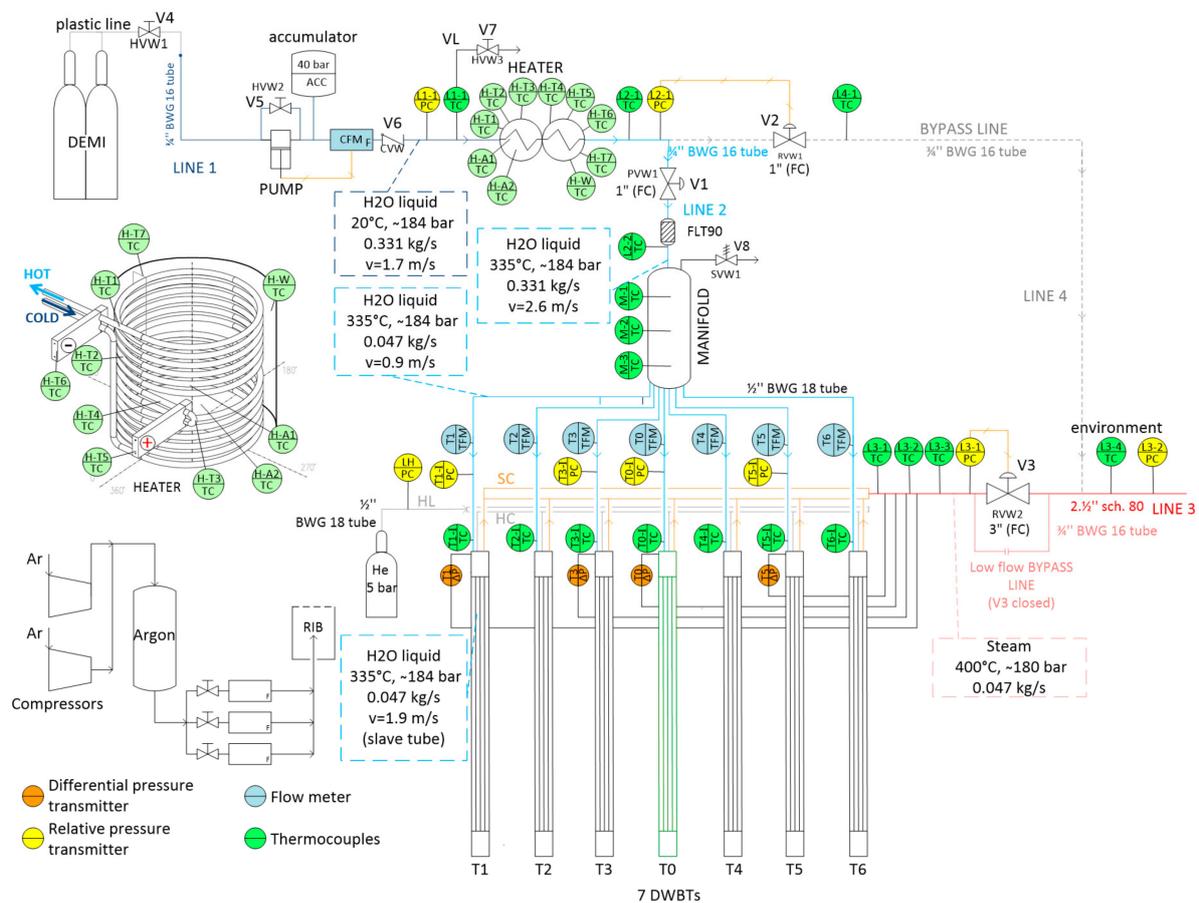
Figure 3. Piping and instrumentation diagram of the HERO SGBT secondary water loop. ACC: Accumulator; CFM: Coriolis Flowmeter; CVW: Check Valve Water; FC: Fail Closed; FLT: Filter; HVW1: Hand Valve Water; PVW: Pneumatic Valve Water; RIB: Riser Bottom; RVW2: Regulation Valve Water; SVW: Safety Valve Water.

3. EUROfusion Experimental Campaign

Within the EUROfusion Work Package Balance of Plant task, an experimental campaign was executed as part of the research activities undertaken at ENEA Brasimone R.C. to investigate the PbLi technology [29–31]. A test matrix of five tests was set up for the CIRCE-HERO facility in order to obtain experimental data in operating conditions relevant for the PbLi/water HEX [12] of the EU DEMO fusion reactor. In the following, the five tests are presented and the main outcomes of the experimental campaign are described. For each test, the boundary conditions to be included in the test matrix were defined by means of a preliminary numerical simulation using the system thermal-hydraulic (STH) code RELAP5-3D$^{\copyright}$ Ver. 4.3.4 [4,32]. Table 1 summarizes the conditions assumed for the five tests. Each test is marked by the initials EF-T, meaning EUROfusion-Test, followed by the test number.

The tests focused attention on the HERO SGBT and its thermal-hydraulic performances. In particular, the component was tested on the basis of the secondary side operating parameters, i.e., pressure, feed water inlet temperature, and flow rate. For this purpose, the secondary system was managed assuming four different values of pressure: 8 MPa in EF-T1, 10 MPa in EF-T2 and EF-T5, 12 MPa in EF-T3, and 6 MPa in EF-T4, kept constant at the HERO outlet section by properly regulating the V3 valve (see Figure 3). These pressure values were selected in order to perform a full characterization of the component

in different operating conditions. At the inlet of the BTs, the feedwater temperature was set by assuring few degrees of sub-cooling respect to the saturation temperature at the corresponding pressure, assuming in such a way the values of 280 °C in EF-T1; 300 °C in EF-T2, EF-T3 and EF-T5; and 250 °C in EF-T4. The water pre-heating was realized by managing the power supplied by the helical heater (see Figure 3). In accordance with the feedwater temperature, the LBE SG inlet temperature was also changed in order to achieve a relevant temperature difference between the primary and secondary coolant, but avoiding at the same time an excessive ΔT along the double wall thickness of the BTs. For these reasons, an LBE temperature of 450 °C was set in EF-T1; 480 °C in EF-T2, EF-T3 and EF-T5; and 430 °C in EF-T4. The LBE temperature at the SG inlet section was kept constant by managing the power supplied by the FPS. Furthermore, an experimental sensitivity analysis was performed by changing the mass flow rate of the LBE (tests EF-T1, EF-T2, EF-T3, and EF-T4) and the flow rate of the feedwater in the steam generator (EF-T5). In particular, the LBE mass flow rate reached an initial value of ~38 kg/s (gas-enhanced circulation regime), from which it was reduced in a total of 5 steps, regulating the properly injected argon flow rate, up to a final value of ~6/~8 kg/s (natural circulation regime). The LBE mass flow rate operating range in the forced circulation regime was selected to reproduce the liquid metal velocities expected in the DCLL BB PbLi/water heat exchangers, which are in the range of 0.5–0.1 m/s. In fact, considering the geometry of the HERO tube bundle and the shell side flow area, the LBE average velocities achieved with the LBE mass flow rate values reported in Table 1 were in the range of 0.15–0.5 m/s. In natural circulation, the LBE velocity field is expected to be lower than 0.1 m/s, thus represening the PbLi flow conditions in the WCLL BB PbLi loop (velocities lower than 0.1 m/s). The EF-T5 focuses the attention on the secondary loop, in particular on the feedwater flow rate, which was decreased from an initial value of ~0.275 kg/s to ~0.175 kg/s in a total of 4 steps. In such a way, it is possible to test the performances of the steam generator when different feedwater flow rates are supplied, evaluating the degree of superheated steam that the component is capable of producing. The experimental conditions reached during the tests are presented in Table 2, which reports the average of the measured values. Details about the LBE mass flow rate average values measured by the VFM and LBE SGBT average inlet temperature are reported in Figure 4, where the x-axes represent the steady states (SS) for each test. The steady state is defined as the time lapse in which the desired test conditions are reached and the main operating parameters (i.e., LBE and water mass flow rates and temperatures, water pressure) remain constant. In EF-T1 and EF-T2, the LBE mass flow rate was in the range of ~38–39 kg/s, whereas it changed from 38.5 kg/s to 4.5 kg/s in EF-T3 and from 30.5 kg/s to 5.5 kg/s in EF-T4. In EF-T5 it was constant at the corresponding designed value of 27 kg/s. Concerning the LBE SGBT inlet temperature, it reached the designed value in EF-T3 and EF-T5, whereas in the other tests it was ~2–4 °C higher than the designed temperatures. A lower value was reached in SS5 of EF-T3, where the LBE average inlet temperature was ~473 °C (see Figure 4b). It can also be observed for the feedwater temperature that in EF-T2 and EF-T3 it was ~4–5 °C lower than the designed values (see Tables 1 and 2), whereas for the other cases it reached the values expected in Table 1. Finally, the water pressure reached the same values of the designed ones for all the tests, and the water flow rate reached values slightly higher in EF-T1 and EF-T2 (difference of 0.02 kg/s) and close to the designed ones in the other tests.

Table 1. Designed boundary conditions for the EUROfusion experiments.

Test ID	LBE m. Flow Rate (kg/s)	LBE Tin SG (°C)	H_2O Flow Rate (kg/s)	H_2O Tin SG (°C)	H_2O Pout SG (MPa)
EF-T1	40/33/27/20/10	450.0	0.31	280	8
EF-T2	40/33/27/20/10	480.0	0.31	300	10
EF-T3	40/33/27/20/10	480.0	0.31	300	12
EF-T4	40/33/27/20/10	430.0	0.31	250	6
EF-T5	27	480.0	0.275/0.245/0.21/0.175	300	10

Table 2. Experimental boundary conditions achieved during the tests.

Test ID	LBE m. Flow Rate (kg/s)	LBE Tin SG (°C)	H$_2$O Flow Rate (kg/s)	H$_2$O Tin SG (°C)	H$_2$O Pout SG (MPa)
EF-T1	37.5/31.5/26.0/20.0/9.0	454	0.33	280.8	8.0
EF-T2	38.3/32.2/27.9/21.0/8.3	483.0	0.33	295.2	10.0
EF-T3	38.5/31.4/24.3/19.6/4.5	480.5	0.32	295.7	12.0
EF-T4	30.5/25.0/19.5/14.0/5.5	432	0.31	250.0	6.0
EF-T5	27.0	480.0	0.28/0.24/0.21/0.17	300.0	10.0
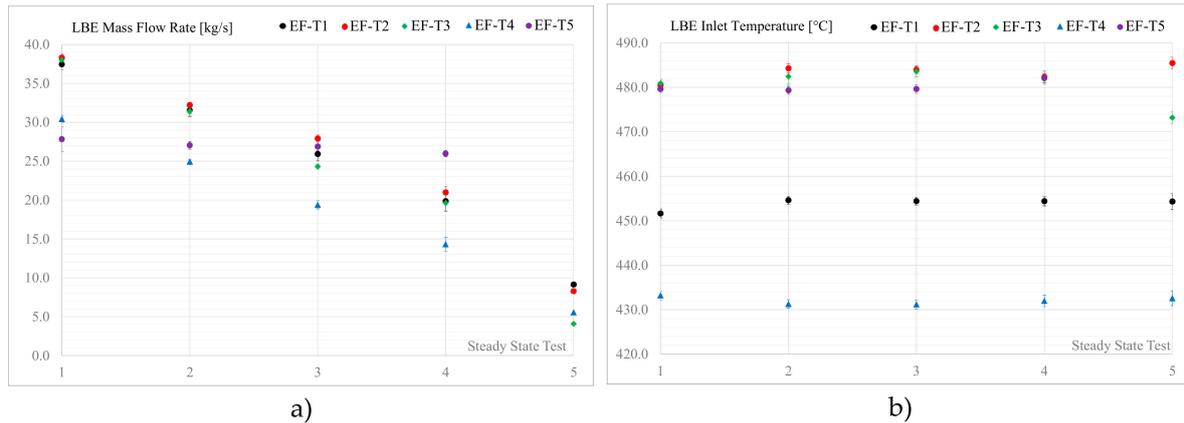
Figure 4. LBE average mass flow rate and relative standard deviation at steady states: (**a**) and LBE average inlet temperature and relative standard deviation at steady states; (**b**) for all the tests.

4. Experimental Tests Results

The experimental outcomes are hereafter presented for all tests and for all steady states, focusing attention on the LBE side of the SG in order to characterize the heat transfer in the liquid metal side and on the water outlet conditions.

4.1. Primary Side Outcomes

The LBE temperatures are reported in Figure 5a, Figure 6a, Figure 7a, Figure 8a, Figure 9a for all the tests and for all the steady states. The figures present the average values of experimental data and the temperature averaged among temperatures measured for each instrumented level (see positions in Figure 2) in order to represent the thermal field along the LBE side of the SG active length. In tests EF-T1 to EF-T4, the LBE outlet temperatures (TC-0X-L00) reached the highest average values during SS1. Then they decreased in the next SSs, coherently with the LBE mass flow rate reduction, achieve the lowest values in SS5. The outlet temperatures achieved in the tests were different because the LBE SGBT inlet temperature was different. In particular, the outlet temperature decreased from ~365 °C (SS1) to ~306 °C (SS5) in EF-T1, from ~390 °C to ~320 °C in EF-T2, from ~392 °C to ~311 °C in EF-T3, and from ~331 °C to ~275 °C in EF-T4. As a consequence, it can be noticed that from SS1 to SS5 there was an increase in the temperature difference between the inlet and the outlet sections of the active length. The ΔT inlet-outlet increased from 86.3 °C (SS1) to 148.7 °C (SS5) in EF-T1, from 84.2 °C to 162.5 °C in EF-T2, from SS1 90 °C to 162.5 °C in EF-T3, and from 98 °C to 162.5 °C in EF-T4. In EF-T5, the LBE average outlet temperature was about 374 °C during SS1, ~364 °C during SS2, ~380 during SS3, and ~382 °C during SS4 (see Figure 9a). The temperature difference between the inlet and outlet of the SG active length was about 100 °C for all the steady states of EF-T5. It can be noticed also that considering the instrumented levels, the LBE temperature difference was smaller among the lower levels (i.e., among 0.0 mm, +1500 mm, +3000 mm, and +4200 mm), whereas it was larger in the higher levels, i.e., between +4200 mm and the SG inlet (6000 mm). These differences along the SG active length were mainly due to the

feedwater, which entered with some degrees of sub-cooling, and this delayed the beginning of the vaporization, which occurred at higher levels. At such levels, thanks to the high efficiency of the vaporization process, the fraction of thermal power removed from the LBE was higher and the LBE temperature differences were larger as a consequence.
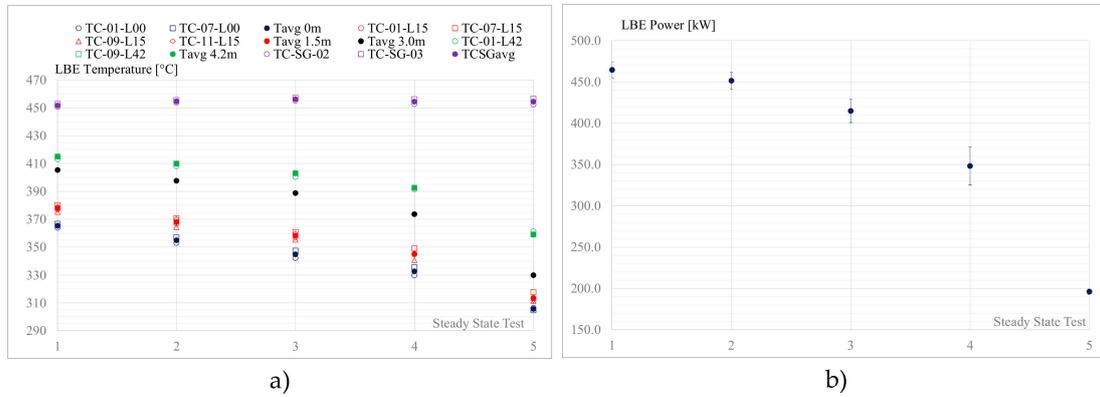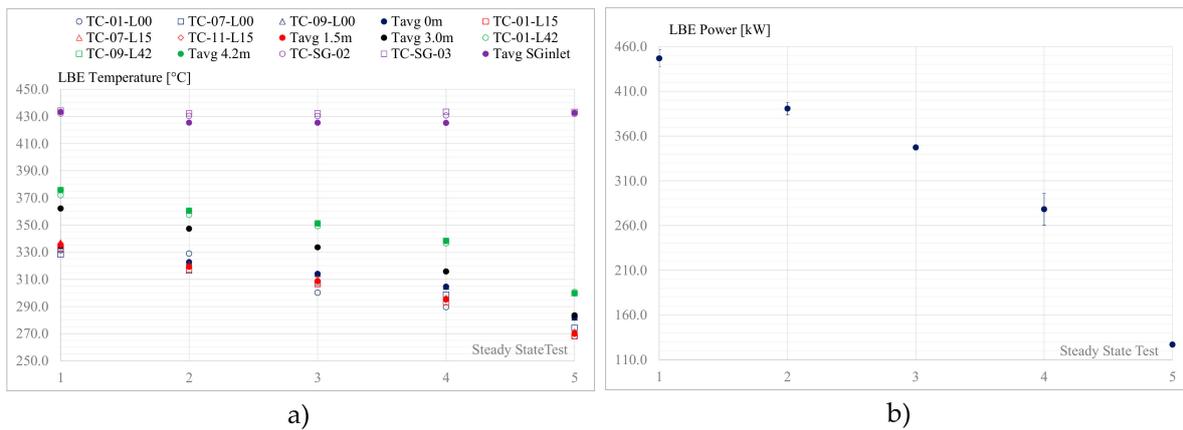

Figure 5. EF-T1: (**a**) LBE temperatures along the SG shell side for all the steady states; (**b**) LBE power and relative standard deviation at steady states.
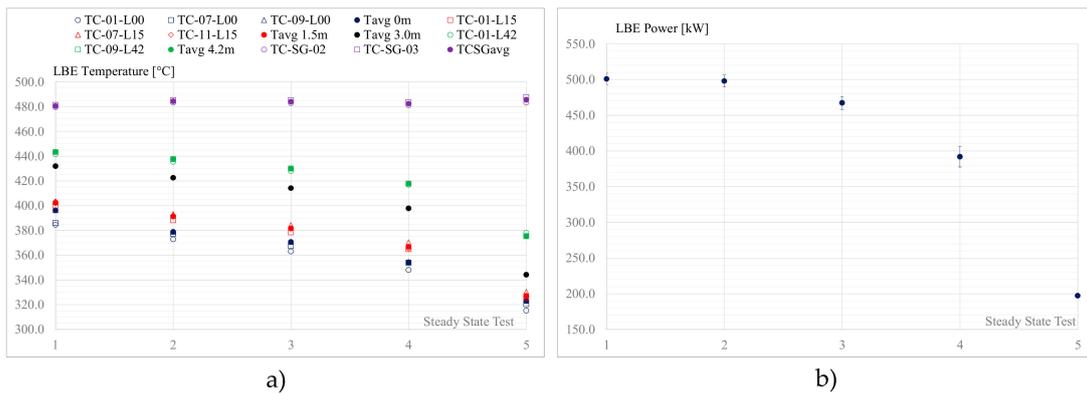
Figure 6. EF-T2: (**a**) LBE temperatures along the SG shell side for all the steady states; (**b**) LBE power and relative standard deviation at steady states.
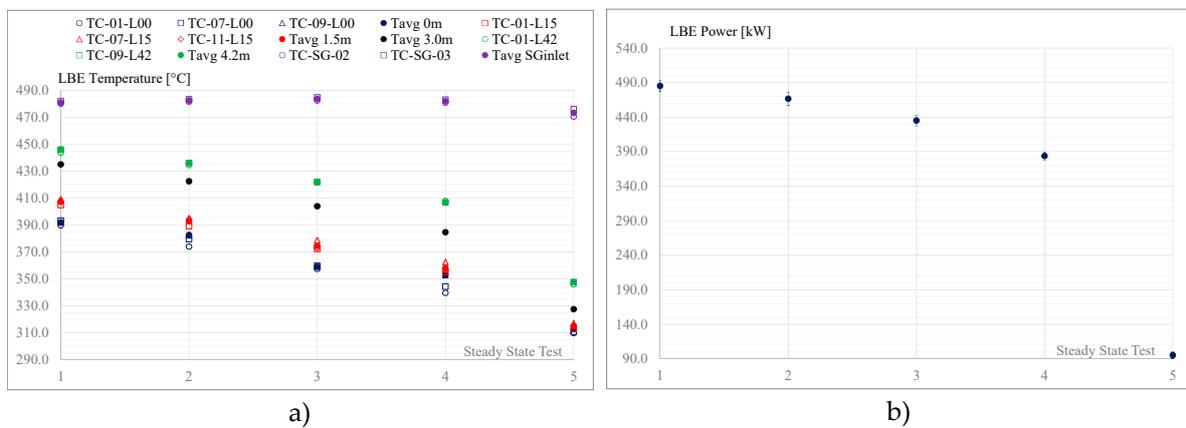
Figure 7. EF-T3: (**a**) LBE temperatures along the SG shell side for all the steady states; (**b**) LBE power and relative standard deviation at steady states.

Figure 8. EF-T4: (**a**) LBE temperatures along the SG shell side for all the steady states; (**b**) LBE power and relative standard deviation at steady states.
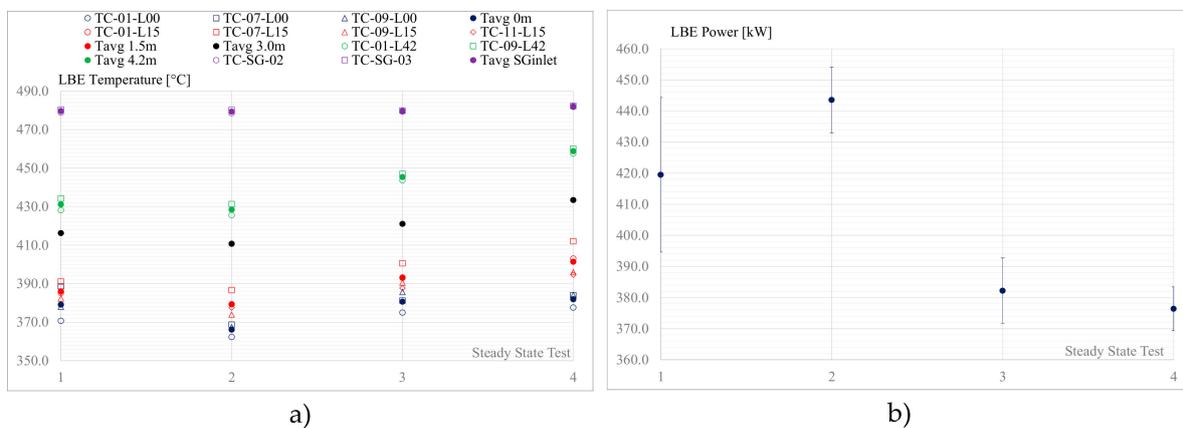

Figure 9. EF-T5: (**a**) LBE temperatures along the SG shell side for all the steady states; (**b**) LBE power and relative standard deviation at steady states.

Taking into account the information on the LBE mass flow rate reported in Table 2 and the LBE temperatures depicted in Figure 5a, Figure 6a, Figure 7a, Figure 8a, Figure 9a, and calculating an average LBE heat capacity using the correlation recommended in [33], it was possible to assess the thermal power exchanged by the SGBT. The thermal balance equation was applied for all steady states of each test. The average values of power obtained are reported in Figure 5b, Figure 6b, Figure 7b, Figure 8b, Figure 9b. From EF-T1 to EF-T4, the fraction of thermal power removed was the highest in SS1, whereas the lowest fraction was achieved in SS5. In particular, the power removed decreased from ~465 kW (SS1) to ~200 kW (SS5) in EF-T1, from ~520 kW to ~200 kW in EF-T2, from ~485 kW to ~100 kW in EF-T3, and from 450 kW to 130 kW in EF-T4. In EF-T5 (Figure 9b), the highest values of thermal power removed were reached during SS1 with ~420 kW and SS2 with ~443 kW, whereas SS3 and SS4 were characterized by a lower power fraction of ~380 KW and 370 kW, respectively.

4.2. Secondary Side Outcomes

Concerning the secondary loop, Figure 10a reports the average temperature at the steam chamber outlet section for all the tests. It can be observed that in all the tests and relative steady states, except for EF-T5, the outlet temperatures reached values equal to or slightly above the saturation temperature corresponding to the operating pressure of each test. This means that in the reproduced operative conditions, the SGBT was capable of producing saturated steam. In EF-T5, the outlet temperature underwent a relevant increase from SS1 to SS4 as consequence of the progressive reduction of the feedwater

flow rate injected in the BTs. SS1 was characterized by an outlet temperature of 318 °C, ~7 °C degrees above the saturation temperature at a pressure of 10 MPa. In the following steady states, the temperature increased to ~337 °C in SS2 and ~390 °C in SS3, up to a final value of ~422 °C in SS4, which was well above the saturation limit of 311 °C. These results prove that the SGBT is capable of reaching high degrees of superheating, producing high temperature steam suitable for the inlet in a turbine.
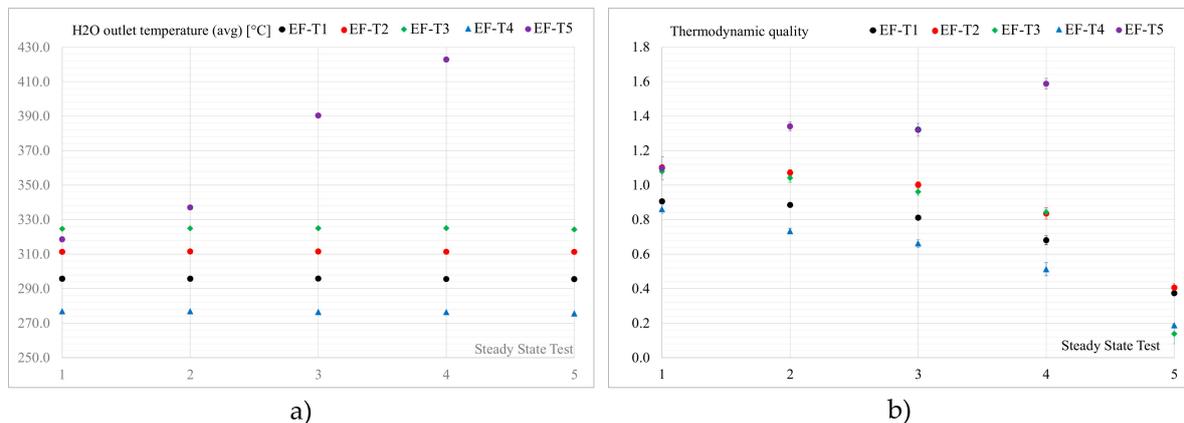
Figure 10. Experimental data at SGBT outlet for all the tests: (**a**) average water temperature and (**b**) thermodynamic quality.

In a two-phase flow system, it is possible to evaluate the thermodynamic quality based on a balance between the specific enthalpy of liquid and steam, respectively, as shown in Equation (1):

$$x_t = \frac{\overline{h} - h_l}{h_v - h_l} \tag{1}$$

where:

- x_t is the thermodynamic quality;
- $\overline{h}$ is the average specific enthalpy of the mixture liquid/steam;
- h_v is the enthalpy of the steam in saturation conditions at the pressure of the system; and
- h_l is the enthalpy of the liquid water in saturation conditions at the pressure of the system.

Since the feedwater inlet conditions (pressure and temperature) are measured during the experiment, h_v and h_l are well defined, whereas $\overline{h}$ can be estimated by applying the thermal balance equation, assuming the power removed from LBE by the secondary coolant and the feedwater flow rate (Table 2) as a reference for the calculations. Figure 10b reports the outcomes of this calculation for all the tests. For EF-T1, in SS1, SS2, and SS3 the highest steam production was achieved (x_t ~0.8/~0.9), whereas SS5 was characterized by a small fraction of steam generated (x_t ~0.4) due to the low thermal power removed from the primary system. The highest values were also achieved in SS1 and SS2 for EF-T2, where x_t was slightly above 1, indicating the complete vaporization of the water, with a slight superheating. SS3 was characterized by a complete vaporization (x_t ~1), whereas in SS4 and SS5 the thermodynamic quality was ~0.85 and ~0.4, respectively. The same values were reached in EF-T3, except for SS5, where the thermodynamic quality was very low (about 0.1). In EF-T4, the values of x_t remained below 1 during all the tests. In SS1 the highest steam production was achieved (x_t ~0.85), then it decreased to ~0.75 in SS2, ~0.65 in SS3, and ~0.5 in SS4, reaching a final value of ~0.2 in SS5. Finally, in EF-T5, the thermodynamic quality x_t was above 1 for all the steady states, proving that the superheated steam was produced by the SGBT for the entire duration of the test. In particular, the initial value in SS1 was about 1.1; then it increased coherently with the feedwater flow rate reduction, reaching the values of ~1.4 in SS2 and SS3 and ~1.6 in SS4.

5. RELAP5 Post-Test Analysis

A numerical model of the secondary system including the SGBT was set up and used to perform a numerical analysis with two versions of the STH code RELAP5: the standard version of RELAP5-3D© Ver. 4.3.4 [17] and a version of RELAP5/Mod3.3 [34], which was modified by implementing the fluid properties of three liquid metals (Pb, LBE, PbLi) and three heat transfer correlations for heavy liquid metals [18,35,36]: Seban–Shimazaki (used for non-bundle geometry) and Ushakov and Mikityuk (used for bundle geometries). The 1-D model includes the SGBT, with the seven double wall BTs modeled separately, the feedwater line, the bypass line, and the discharge line [13]. Each BT consists of a single pipe component simulating the slave tube, and an annulus component, which represents the annular region between first tube and second tube. Furthermore, an equivalent single pipe simulates the LBE shell side of steam generator. The water and LBE inlet thermodynamic conditions and the environmental conditions for the steam discharge are defined using time-dependent volumes, whereas water and LBE mass flow rate are set by means of time-dependent junctions. The spatial division of the SG and secondary system components was realized by taking into account the correct positions of the instrumentation placed along the loop, as well as the wall and bulk TCs installed in the active length of the SGBT. The full nodalization can be found in [16].

Dedicated heat structures simulate the thermal coupling between the annular riser of each BT and the LBE equivalent channel. Standard RELAP5-3D uses the Westinghouse correlation for liquid metal convective heat transfer in the HERO tube bundle zone [37,38], whereas the Ushakov correlation is used in RELAP5/Mod3.3. The BT downcomer was instead assumed to be thermally insulated with respect to the annulus. The feeding line, bypass line and discharge line were also assumed to be thermally insulated. The water warm-up inside the helical pre-heater was simulated by introducing an additional heat structure, which reproduced a heating source uniformly distributed along the helical pipe length, as well as along the pipe thickness.

For the validation purpose, the analysis presented in this section is focused on the heat transfer within the liquid metal side of the SGBT, comparing the computational outcomes with the experimental data acquired on the primary side of the TS.

For the simulation of each test, the experimental boundary conditions reported in Table 2 were assumed in the input deck. In particular, LBE and water mass flow rates were assumed by considering the measurements of the VFM and the TFMs, respectively. The temperatures at the HERO SG inlet section were assumed by considering the average of the temperatures measured by the TC-SG-0X for the LBE and TC-TX-I for the water. Finally, the pressure at the outlet section of the secondary loop was assumed constant for the duration of each test and set equal to the measure of PC-L3-1.

First, the RELAP5-3D results were compared with the average values of the experimental temperatures obtained along the LBE side of the SG and the wall temperatures for all tests and steady states.

The results of the LBE temperature for all the tests are reported in Figure 11a, Figure 12a, Figure 13a, Figure 14a, Figure 15a. The results show that, in general, the code predicted the LBE temperature with good accuracy, as minor differences were observed between the numerical values and the average experimental acquisition. A discrepancy was found in SS4 of EF-T3 and SS4 of EF-T5, where RELAP5-3D code overestimated the experimental temperatures of ~10/~15 °C. It was also observed in EF-T4 that the temperatures were overestimated by the code, about ~10/~20 °C. Such discrepancies were probably due to an unbalanced distribution of the LBE flow in the sub-channels, which could not be reproduced by the numerical model since it simulates the LBE channels with a single 1-D equivalent pipe.

The comparison between the measured wall temperatures and RELAP5-3D results are presented in Figure 11b, Figure 12b, Figure 13b, Figure 14b, Figure 15b. It can be observed that in all the instrumented sections the wall temperatures were ~10/~20 °C lower than the LBE sub-channel temperatures. This difference was clearly visible in SS1, SS2, SS3,

and SS4, whereas in SS5 the difference was less pronounced because of the low LBE mass flow rate, and thus a low velocity, which led to a more homogeneous radial thermal field. The differences in temperatures between the LBE and wall tubes were also predicted by the RELAP5-3D results. Nevertheless, the comparison between the experimental and numerical values demonstrates that there was a difference between the results because the code underestimated the temperature. The RELAP5-3D code underestimated the temperatures by ~15/~20 °C in EF-T1, EF-T2, and EF-T4. In EF-T3, the RELAP5-3D temperatures were generally lower than the experimental values and minor differences were observed, with the exception of SS3 and SS4 at section +1500 mm, where the RELAP5-3D value was greater than the experimental value of ~10 °C. This last discrepancy was probably due to a not-uniform LBE flow distribution among the sub-channels. As already mentioned, the numerical model simulates the LBE channel with a 1-D equivalent pipe. This means that the sub-channels effects are not reproduced and the resultant thermo-hydraulic behavior is a consequence of the averaged values. Finally, in EF-T5, the wall temperatures calculated by RELAP5-3D were in agreement with the measured ones, except in SS1, where the code underestimated the wall temperature by ~20 °C.
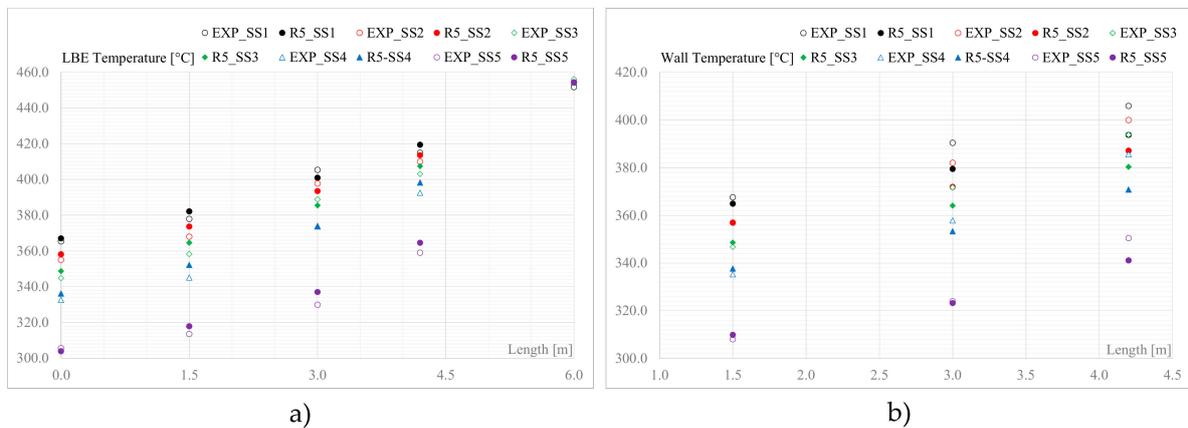
Figure 11. EF-T1, exp. vs. RELAP5-3D: (**a**) SG LBE bulk temperatures; (**b**) wall temperatures.
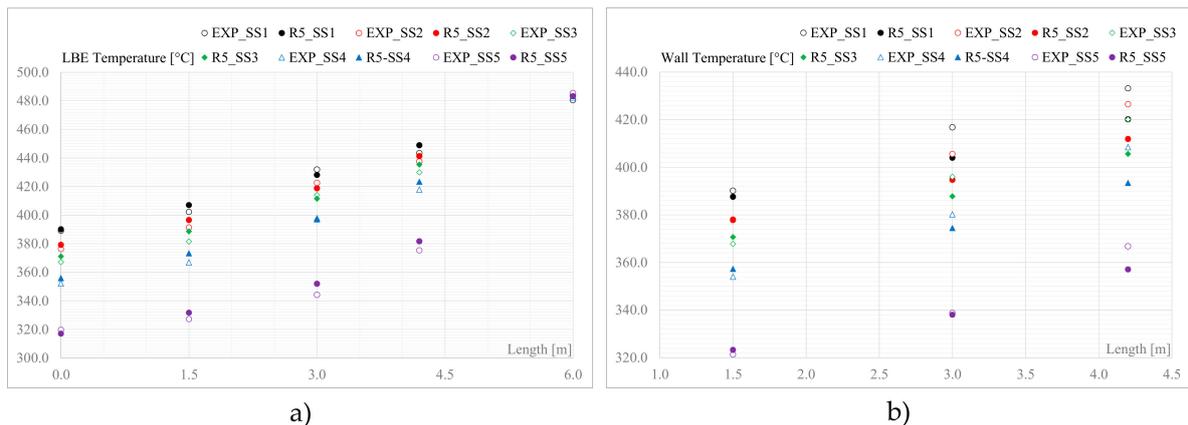
Figure 12. EF-T2, exp. vs. RELAP5-3D: (**a**) SG LBE bulk temperatures; (**b**) wall temperatures.

The discrepancies between the experimental and numerical wall temperatures could be addressed to the simplified model, which uses an LBE equivalent pipe, and could not reproduce the sub-channel effects. Other reasons could be the uncertainty related to the acquisition of the experimental measurements, eventual unbalanced distribution of the LBE flow rate in the sub-channels and feedwater among the seven bayonet tubes [25], as well as the uncertainty related to the heat transfer correlations used by RELAP5-3D.
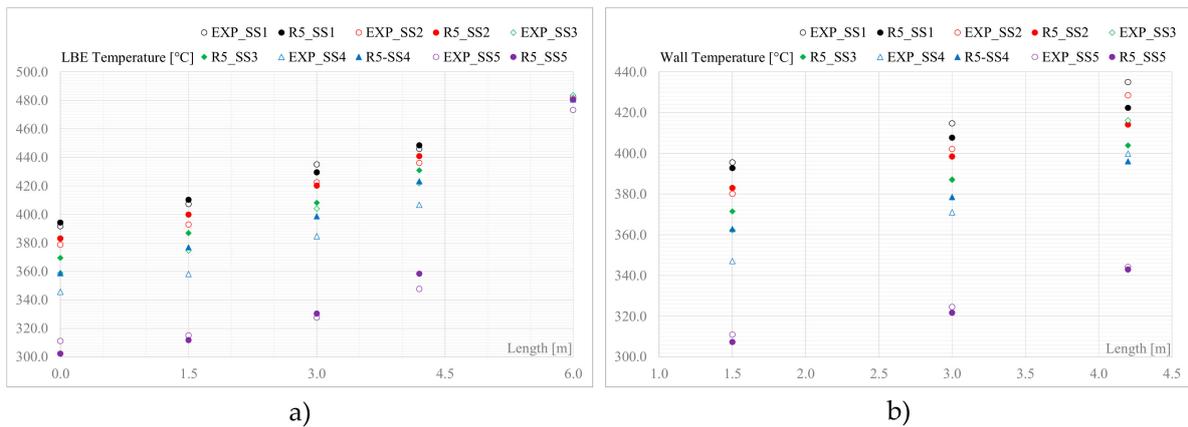
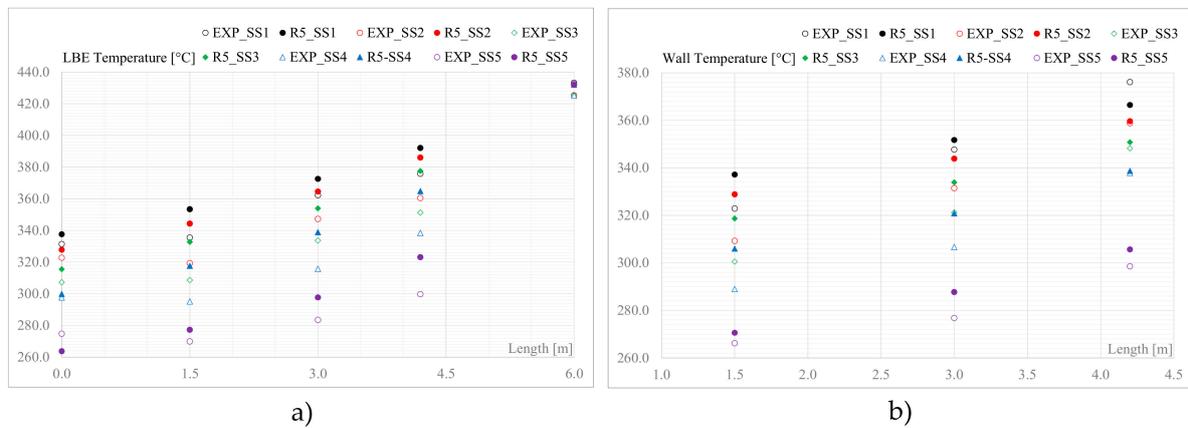**Figure 13.** EF-T3, exp. vs. RELAP5-3D: (**a**) SG LBE bulk temperatures; (**b**) wall temperatures.

Figure 14. EF-T4, exp. vs. RELAP5-3D: (**a**) SG LBE bulk temperatures; (**b**) wall temperatures.
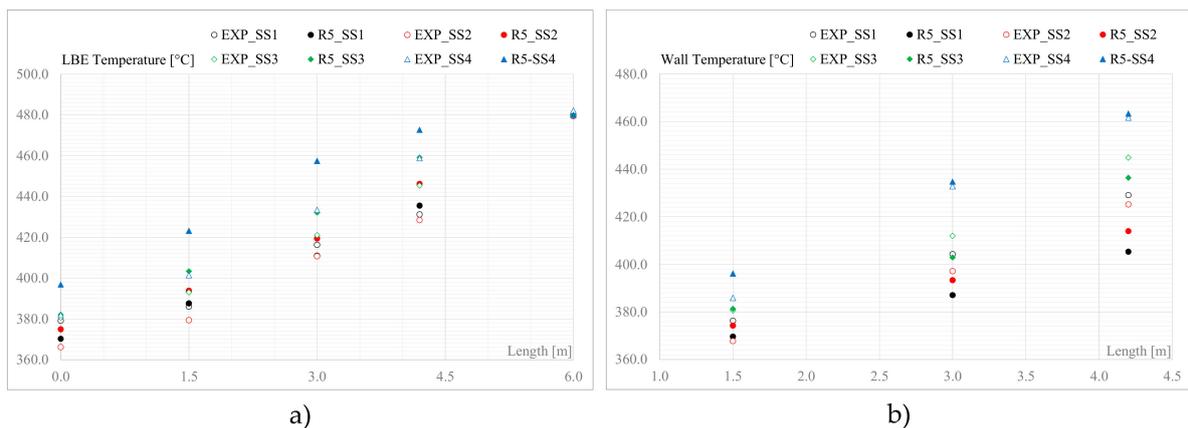
Figure 15. EF-T5, exp. vs. RELAP5-3D: (**a**) SG LBE bulk temperatures; (**b**) wall temperatures.

The thermal conductivity of the HERO double-wall gap could also be a source of uncertainty. In fact, the thermal conductivity of the AISI316L powder + He used to fill the gap is a function of the temperature and is influenced by several factors, i.e., powder compaction, grain size and growth, and thermal cycling [39]. Dedicated experimental campaigns performed at ENEA Brasimone R.C. allowed the experimental correlations reported in [40] to be derived. Such correlations were taken as reference for the simulations since they were used for the HERO SGBT design.

Finally, during the operation of the system, the LBE coolant may have formed compounds that attached to the outer surface of the tubes composing the HERO bundle. This could have caused an additional thermal resistance [41], which could have enlarged the discrepancies between the experimental and numerical outcomes. Nevertheless, this hypothesis can be verified only with a direct inspection during the next refurbishment of the facility.

The same simulations were performed using RELAP5/Mod3.3 in order to compare the performances of the codes. The results of the simulations were compared with the RELAP5-3D outcomes in Table 3 for all the steady states of EF-T3 in terms of the LBE temperatures and wall temperatures along the SG shell side.

Table 3. EF-T3: RELAP5-3D/RELAP5/Mod3.3 (in bold) simulation results comparison.

		R5-3D Simulation Results						
		R5-Mod3.3 Simulation Results						
		Coolant Temperature SG [°C]				Wall Temperature [°C]		
EF-T#	SS_#	+4200 mm	+3000 mm	+1500 mm	Out	+4200 mm	+3000 mm	+1500 mm
EF-T3	SS_1	448.4	429.5	410.3	394.3	422.3	407.6	392.7
		447.4	**428.2**	**408.9**	**392.7**	**422.1**	**407.2**	**392.0**
	SS_2	440.8	420.1	399.8	383.1	414.0	398.4	383.0
		439.8	**418.8**	**398.4**	**381.6**	**413.9**	**398.0**	**382.3**
	SS_3	430.9	408.1	386.9	369.5	403.8	387.1	371.5
		429.7	**406.7**	**385.4**	**367.9**	**403.7**	**386.6**	**370.8**
	SS_4	423.2	398.6	376.9	358.8	396.0	378.5	362.8
		422.0	**397.2**	**375.5**	**357.4**	**396.0**	**378.1**	**362.3**
	SS_5	358.4	330.5	311.8	302.4	342.9	321.7	307.3
		356.0	**328.4**	**310.5**	**301.6**	**341.8**	**320.5**	**306.5**

The results demonstrate that there was good agreement between the two codes. Small discrepancies of ~0.5 °C/~1.5 °C between codes can be observed due to the different heat transfer correlations used (i.e., Westinghouse correlation for RELAP5-3D and Ushakov correlation for RELAP5/Mod3.3) and the fact that the RELAP5/Mod3.3 code considers the reference properties of the LBE reported in [33], which were updated respective to those available in RELAP5-3D [17]. The comparison presented in Table 3 is representative of the ones carried out for all the other tests.

6. Analysis of the Experimental Data in Case of PbLi Working Fluid

The CIRCE experimental facility, and thus the steam generator test section, uses LBE as primary fluid, whereas PbLi is the fluid selected for applications in DEMO. It should be noted that both fluids rely on the same formulations of the Nusselt number. Therefore, the following sections report an analysis of the correspondence between LBE and PbLi, preserving the convective heat transfer (method #1) and both the thermal power and temperature difference (method #2).

6.1. Method #1

Method #1 aims to maintain the same conditions of convective heat transfer across the active length of the SG, preserving the Nusselt number. This condition can be satisfied by changing the experimental mass flow rate, taking into account the thermo-physical differences between LBE and PbLi. The reference parameter to apply this method is the Peclet number. First, the Peclet number was evaluated for each test from the available experimental data. The LBE density, thermal conductivity, and heat capacity were calculated on the basis of the LBE average temperature and in accordance with the correlations

reported in [33]. Then the Peclet number was calculated. The same parameters (density, thermal conductivity, and heat capacity) were also calculated, considering the PbLi as the working fluid. Assuming the same values as the Peclet, it was possible to recalculate the equivalent theoretical PbLi mass flow rate as reported in Table 4.

Table 4. CIRCE-HERO EF-T1 and EF-T2: equivalence between LBE and PbLi using method #1, preserving the Peclet number and Nusselt number: experimental vs. RELAP5-3D results.

ID	*W*	*Pe* LBE	*mf* PbLi	*v* PbLi	*Nu* Exp	*Nu* PbLi R5-3D	Error
	[kW]	—-	[kg/s]	[m/s]	—-	—-	[%]
T1_SS1	464.4	1387.48	32.5	0.44	16.93	21.36	26.1
T1_SS2	451.4	1172.43	27.4	0.37	15.31	19.49	27.3
T1_SS3	414.8	973.46	22.8	0.31	13.78	17.71	28.5
T1_SS4	348.2	754.16	17.6	0.24	12.03	15.66	30.2
T1_SS5	196.1	344.82	8.1	0.11	8.55	11.43	33.6
T2_SS1	521	1367	32.0	0.43	16.78	20.84	24.1
T2_SS2	504.7	1158	27.1	0.36	15.20	19.79	30.1
T2_SS3	474.2	1019	23.8	0.32	14.13	18.46	30.6
T2_SS4	395.3	770	18.0	0.24	12.16	16.04	31.8
T2_SS5	199.4	299	7.0	0.09	8.13	11.24	38.2

A new RELAP5-3D run was set using the model introduced in Section 5 and running the calculation using the PbLi as the working fluid. Unlike the liquid metal mass flow rate, the initial and boundary conditions of the simulations corresponded to those summarized in Table 2.

The simulation outcomes are presented in Table 4, in which the experimental and RELAP5-3D Nusselt numbers are compared for EF-T1 and EF-T2. The *Nu* was calculated with the heat transfer correlation used for liquid metals in a rod bundle (Westinghouse correlation):

$$Nu = 4.0 + 0.33(P/D)^{3.8}(Pe/100)^{0.86} + 0.16(P/D)^5, \tag{2}$$

where

- *Nu* is the Nusselt number;
- *P/D* is the pitch-to-diameter ratio (in HERO geometry, *P/D* = 1.42) of the rods; and
- *Pe* is the Peclet number.

Comparing the experimental and computed values, it emerged that the errors were in range of 26.1–33.6% for EF-T1 and 24.1–38.2% for EF-T2. These discrepancies could be partially due to the uncertainty related to the use of Equation (2) for the calculation of *Nu* and to the differences between the thermo-physical proprieties of RELAP5-3D (i.e., c_p = 180.5 J/kgK at 400 °C) and the most updated values in [42] (i.e., c_p = 187.8 J/kgK at 400 °C). Neglecting the contribution of the fluid properties, the errors decreased in the range of 18–29% for EF-T1 and 15.7–28.7% for EF-T2. Similar differences were found by applying the scaling method #1 to the other tests.

6.2. Method #2

This method preserves the power exchanged and the difference of temperature across the SG. The experimental mass flow rate is changed considering the thermo-physical differences between LBE and PbLi. The reference parameter considered for the correspondence is the heat capacity. The PbLi mass flow rate (see Table 5) was re-calculated and used as a boundary condition to perform simulations with RELAP5-3D, using PbLi as the working

fluid. In this way it was possible to compare the experimental data with the simulations involving PbLi.

Table 5. CIRCE-HERO EF-T1 and EF-T2, equivalence between LBE and PbLi using method #2, preserving power and temperatures: experimental vs. RELAP5-3D results.

Test ID	W	DT_{exp} LBE	c_p _PbLi	mf_pbli	Tin	T_{exp} Out	T R5-3D PbLi Out	Error
—-	(kW)	(°C)	(J/kgK)	(kg/s)	(°C)	(°C)	(°C)	(°C)
T1_SS1	464.4	88.9	187.8	27.8	454.2	365.3	360.1	5.1
T1_SS2	451.4	99.2	187.8	24.2	454.2	355	350.7	4.2
T1_SS3	414.8	109.4	187.8	20.2	454.2	344.8	340.9	3.8
T1_SS4	348.2	121.6	187.8	15.2	454.2	332.6	328.1	4.4
T1_SS5	196.1	148.6	187.8	7.0	454.2	305.6	297.7	7.8
T2_SS1	521	97.9	187.8	28.3	483.3	385.4	382.6	6.4
T2_SS2	504.7	108.4	187.8	24.8	483.3	374.9	371.1	3.8
T2_SS3	474.2	118.1	187.8	21.4	483.3	365.2	362.8	2.4
T2_SS4	395.3	132.3	187.8	15.9	483.3	351	347.2	3.8
T2_SS5	199.4	165.4	187.8	6.4	483.3	317.9	310.7	7.2

The simulation results are summarized in Table 5, where they are compared with the LBE temperatures at the SGBT outlet section in EF-T1 and EF-T2. Absolute errors were within the range of 3.8–7.8 °C for EF-T1 and in the range of 2.4–7.2 °C for EF-T2. Taking into account the thermo-physical propriety differences between the ones from RELAP5-3D and the most updated values in [42], the expected discrepancies in the calculation of the outlet temperatures were in the range of ~4–6 °C. This implies that, neglecting this contribution, the errors became consistent with the uncertainty of the experimental measurements. Similar differences were found by applying scaling method #2 to the other tests.

7. Conclusions

Within the R&D program for the DEMO development, a research activity was addressed to develop a PbLi/water HEX capable of efficiently removing the thermal power from the DCLL BB and for the PbLi loop of the WCLL BB. An experimental and numerical investigation was performed involving the HERO SGBT at ENEA Brasimone R.C. with the aim of investigating the thermal-hydraulic characteristics of the component, improving the knowledge and the experience in terms of design and operations, and providing an experimental database to support the validation process of numerical tools. The paper describes five characterization tests in which the HERO SGBT was involved in the pool-type LBE-cooled facility CIRCE. The results of the research activity led to the following conclusions:

- During each test, the steady state conditions and the designed boundary conditions needed to test the SG were achieved. In the LBE side (primary side), the FPS managed to supply the thermal power necessary to balance the power removed by the SGBT and the fraction of power lost from the CIRCE pool toward the environment, keeping the LBE temperature at the SG inlet section as close as possible to the target values (maximum discrepancy ~4 °C).
- A dedicated argon injection device was used to perform a gas-enhanced circulation regime, achieving the designed values of LBE mass flow rate in each SS. Small discrepancies were observed in some cases, where the experimental LBE mass flow rate achieved was lower than the designed values. The average velocity of the LBE along

the shell side of the SGBT was in the range of 0.5 m/s (EF-T1, SS1) and 0.05 m/s (EF-T3, SS5) and this was coherent with the PbLi velocities expected in the DCLL BB PbLi loop (for velocities in range 0.5–0.1 m/s) and the WCLL BB PbLi loop (velocity lower than 0.1 m/s).

- A secondary loop was realized in order to feed the HERO SGBT. The main components (i.e., volumetric pump, regulation valves, helical heater) were managed in order to achieve the water conditions foreseen for the tests.

- At the SG outlet, the LBE temperatures reached the maximum average values during SS1 of each test. Then they decreased in the following steady states, in accordance with the LBE mass flow rates reduction, and achieved the minimum values during SS5.

- In EF-T5 the steam outlet temperature was well above the saturation limit of 311 °C (i.e., ~337 °C in SS2 and ~390 °C in SS3, up to the final value of ~422 °C in SS4). These results demonstrate that the SGBT is capable of reaching high degrees of superheating, producing high temperature steam suitable for the inlet in a turbine.

- The thermal power removed by HERO for each SS and for all the tests was assessed by applying the thermal balance equation: The highest fraction was achieved in EF-T2-SS1 (~520 kW), whereas the lowest fraction was achieved in EF-T3-SS5 (~100 kW).

- A numerical post-test analysis using the STH codes RELAP5-3D$^{©}$ Ver. 4.3.4 and RELAP5/Mod3.3 was performed by exploiting the outcomes of the experimental tests. Both versions of the code were demonstrated to have the capability to simulate this type of component, in particular as regards the liquid metal side. Minor differences (~0.5–1.5 °C) were observed between the two codes. The most relevant discrepancies were observed from the comparison of the SGBT wall temperatures calculated by the codes and the experimental ones. The reasons for such discrepancies could be found in the numerical model setup, which could not reproduce the LBE sub-channel effects and possible unbalance in the LBE flow. The analysis of the results also highlighted a possible source of uncertainty in the powder + He gap and its thermal conductivity, which was influenced by different factors (i.e., powder compaction, grain size and growth, thermal cycling) during the HERO SGBT operation. The eventual formation of LBE compounds around the HERO tubes and the consequent increase of thermal resistance could also enhance such discrepancies. Verification of this last hypothesis will be made when the HERO SGBT is dismantled.

- Two scaling analysis approaches were proposed to find an equivalence between LBE and PbLi. RELAP5-3D code was applied to recalculate the data of the experiments using PbLi as the working fluid. Considering method #1, which preserves the convective heat transfer, and comparing experimental and calculated values, it emerged that the errors in terms of Nu were in the range of 26.1–33.6% for EF-T1 and 24.1–38.2% for EF-T2. These discrepancies could be partially due to the uncertainty related to the correlation used by RELAP5-3D for the calculation of Nu and to the differences of the thermo-physical proprieties between the ones from RELAP5-3D and the most updated values. Neglecting the contribution of the fluid properties, the errors decreased in the range of 18–29% for EF-T1 and 15.7–28.7% for EF-T2. Considering method #2 and thus preserving the thermal power and the difference of temperature, the code predicted differences in the range of 4–6 °C on the outlet temperatures, thus neglecting the contribution of the PbLi properties. The errors of the code results were in range of −1.8 °C and 0.6 °C. The same differences were found by applying the scaling methods to the other tests. Of the two methods, method #2 seemed to be more appropriate for the purposes of the present activity, since it preserved the thermal power exchanged, and thus the main figure of merit, which represented the efficiency of the component.

In conclusion, the activity carried out highlighted that the component has good capability to remove the thermal power from liquid metal, producing at the same time high quality steam suitable for feeding a steam turbine unit. The good efficiency, combined with the enhanced safety features given by the double wall tubes, make the SGBT concept suitable for DEMO purposes.

Institutional Review Board Statement: Not applicable.

Informed Consent Statement: Not applicable.

Data Availability Statement: Not applicable.

Conflicts of Interest: The authors declare no conflict of interest. The funders had no role in the design of the study; in the collection, analyses, or interpretation of data; in the writing of the manuscript, or in the decision to publish the results.

Abbreviations

BB	breeding blanket
BT	bayonet tube
CIRCE	CIRColazione Eutettico
DCLL	dual coolant lithium lead
EF-T	EUROfusion-Test
ENEA	Agenzia nazionale per le nuove tecnologie, l'energia e lo sviluppo economico sostenibile
FPS	fuel pin simulator
HERO	Heavy Liquid mEtal pRessurized water cOoled tubes
HEX	heat exchanger
LBE	lead–bismuth eutectic
Nu	Nusselt number
PbLi	lithium–lead
Pe	Peclet number
P&ID	procedures and instrumentation description
RC	Research Centre
SG	steam generator
SGBT	steam generator bayonet tube
SS	steady state
STH	system thermal-hydraulic
TC	thermocouple
TFM	turbine flow meter
TS	test section
VFM	Venturi flow meter
WCLL	water cooled lithium lead

References

1. Boccaccini, L.; Aiello, G.; Aubert, J.; Bachmann, C.; Barrett, T.; Del Nevo, A.; Demange, D.; Forest, L.; Hernandez, F.; Norajitra, P.; et al. Objectives and status of EUROfusion DEMO blanket studies. *Fusion Eng. Des.* **2016**, *109–111*, 1199–1206. [CrossRef]
2. Rapisarda, D.; Fernández-Berceruelo, I.; Palermo, I.; Urgorri, F.R.; Maqueda, L.; Alonso, D.; Melichar, T.; Frýbort, O.; Vála, L.; González, M.; et al. Status of the engineering activities carried out on the European DCLL. *Fusion Eng. Des.* **2017**, *124*, 876–881. [CrossRef]
3. Del Nevo, A.; Arena, P.; Caruso, G.; Chiovaro, P.; Di Maio, P.A.; Eboli, M.; Edemetti, F.; Forgione, N.; Forte, R.; Froio, A.; et al. Recent progress in developing a feasible and integrated conceptual design of the WCLL BB in EUROfusion project. *Fusion Eng. Des.* **2019**, *146*, 1805–1809. [CrossRef]

4. Martelli, E.; Del Nevo, A.; Lorusso, P.; Giannetti, F.; Narcisi, V. *Conceptual Design of a PbLi/Water Heat Exchanger and Design of the Experimental Campaign*; EC H2020 EUROfusion Project, WPBoP BOP-4.1.1-T001-D001, IDM Ref. 2N3VXE v1.0; European Commission: Brussels, Belgium, 10 April 2019.

5. Eboli, M.; Moghanaki, S.K.; Martelli, D.; Forgione, N.; Porfiri, M.T.; Del Nevo, A. Experimental activities for in-box LOCA of WCLL BB in LIFUS5/Mod3 facility. *Fusion Eng. Des.* **2019**, *146*, 914–919. [CrossRef]

6. Di Maio, P.A.; Arena, P.; D'Aleo, F.; Del Nevo, A.; Eboli, M.; Forte, R.; Pesetti, A. Thermal-hydraulic and thermo-mechanical simulations of Water-Heavy Liquid Metal interactions towards the DEMO WCLL breeding blanket design. *Fusion Eng. Des.* **2019**, *146*, 2712–2716. [CrossRef]

7. Eboli, M.; Del Nevo, A.; Pesetti, A.; Forgione, N.; Sardain, P. Simulation study of pressure trends in the case of loss of coolant accident in Water Cooled Lithium Lead blanket module. *Fusion Eng. Des.* **2015**, *98–99*, 1763–1766. [CrossRef]

8. DeFur, D.D. *LMFBR Steam Generator Development: Duplex Bayonet Tube Steam Generator Volume II*; CENC1238; Combustion Engineering Incorporated: Chattanooga, TN, USA, 1975. [CrossRef]

9. Caramello, M.; Gregorini, M.; Bertani, C.; De Salve, M.; Alemberti, A.; Panella, B. Thermal hydraulic analysis of a passively controlled DHR system. *Prog. Nucl. Energy* **2017**, *99*, 127–139. [CrossRef]

10. Narcisi, V.; Giannetti, F.; Caramello, M.; Caruso, G. Preliminary evaluation of ALFRED revised concept under station blackout. *Nucl. Eng. Des.* **2020**, *364*, 110648. [CrossRef]

11. Alemberti, A.; Caramello, M.; Frignani, M.; Grasso, G.; Merli, F.; Morresi, G.; Tarantino, M. ALFRED reactor coolant system design. *Nucl. Eng. Des.* **2020**, *370*, 110884. [CrossRef]

12. Lorusso, P.; Martelli, E.; Del Nevo, A.; Tarantino, M. *PbLi Heat Exchanger and Fluid Technology—As built PbLi/H2O HX Test Facility Report*; EC H2020 EUROfusion Project, WPBOP-4-T002-D001, IDM Ref. 2N6K97 v1.2; European Commission: Brussels, Belgium, 3 October 2019.

13. Martelli, E.; Del Nevo, A.; Lorusso, P.; Giannetti, F.; Narcisi, V.; Tarantino, M. Investigation of heat transfer in a steam generator bayonet tube for the development of PbLi technology for EU DEMO fusion reactor. *Fusion Eng. Des.* **2020**, *159*, 111772. [CrossRef]

14. Lorusso, P.; Martelli, E.; Del Nevo, N.V.; Giannetti, F. Development of a PbLi heat exchanger for EU DEMO fusion reactor: Experimental test and system code assessment. In Proceedings of the 31st Symposium on Fusion Technology (SOFT2020), Virtual Conference. Dubrovnik, Croatia, 20–25 September 2020.

15. Lorusso, P.; Pesetti, A.; Tarantino, M. ALFRED steam generator assessment: Design and pre-test analysis of HERO experiment. In *Volume 6B: Thermal-Hydraulics and Safety Analyses, Proceedings of the 2018 26th International Conference on Nuclear Engineering, London, UK, 22–26 July 2018*; ASME: New York, NY, USA, 2018. [CrossRef]

16. Lorusso, P.; Tarantino, M.; Pesetti, A.; Narcisi, V. Protected loss of flow accident simulation in CIRCE-HERO facility: Experimental test and system code assessment. In Proceedings of the 27th International Conference on Nuclear Engineering (ICONE 2019), Tsukuba, Japan, 19–24 May 2019. paper 150404.

17. The RELAP5-3D Code Development Team. *RELAP5-3D© Code Manual*; Idaho National Engineering Laboratory, Lockheed-Martin Idaho Technologies Company: Idaho Falls, ID, USA, 2013; INEEL-EXT-98-00834. Available online: https://relap53d.inl.gov/SitePages/RELAP5-3D%20Manuals.aspx (accessed on 22 January 2021).

18. Martelli, E.; Giannetti, F.; Ciurluini, C.; Caruso, G.; Del Nevo, A. Thermal-hydraulic modeling and analyses of the water-cooled EU DEMO using RELAP5 system code. *Fusion Eng. Des.* **2019**, *146*, 1121–1125. [CrossRef]

19. Martelli, E.; Giannetti, F.; Caruso, G.; Tarallo, A.; Polidori, M.; Barucca, L.; Del Nevo, A. Study of EU DEMO WCLL breeding blanket and primary heat transfer system integration. *Fusion Eng. Des.* **2018**, *136*, 828–833. [CrossRef]

20. Lorusso, P.; Bassini, S.; Del Nevo, A.; Di Piazza, I.; Giannetti, F.; Tarantino, M.; Utili, M. GEN-IV LFR development: Status and perspectives. *Prog. Nucl. Energy* **2018**, *105*, 318–331. [CrossRef]

21. Tarantino, M.; Agostini, P.; Benamati, G.; Coccoluto, G.; Gaggini, P.; Labanti, V.; Venturi, G.; Class, A.; Liftin, K.; Forgione, N.; et al. Integral circulation experiment: Thermal–hydraulic simulator of a heavy liquid metal reactor. *J. Nucl. Mater.* **2011**, *415*, 433–448. [CrossRef]

22. Lorusso, P.; Pesetti, A.; Tarantino, M.; Narcisi, V.; Giannetti, F.; Forgione, N.; Del Nevo, A. Experimental analysis of stationary and transient scenarios of alfred steam generator bayonet tube in circe-hero facility. *Nucl. Eng. Des.* **2019**, *352*, 110169. [CrossRef]

23. Lorusso, P.; Pesetti, A.; Barone, G.; Castelliti, D.; Caruso, G.; Forgione, N.; Giannetti, F.; Martelli, D.; Rozzia, D.; Van Tichelen, K.; et al. MYRRHA primary heat exchanger experimental simulations on CIRCE-HERO. *Nucl. Eng. Des.* **2019**, *353*. [CrossRef]

24. Castelliti, D.; Hamidouche, T.; Lorusso, P.; Tarantino, M. H2020 MYRTE CIRCE-HERO experimental campaign post-test activity and code validation. In Proceedings of the 18th International Topical Meeting on Nuclear Reactor Thermal Hydraulics (NURETH-18), Portland, OR, USA, 18–23 August 2019.

25. Narcisi, V.; Giannetti, F.; Del Nevo, A.; Tarantino, M.; Caruso, G. Post-test simulation of a PLOFA transient test in the CIRCE-HERO facility. *Nucl. Eng. Des.* **2019**, *355*, 110321. [CrossRef]

26. Francesco, G.; Barone, G.; Martelli, D.; Pucciarelli, A.; Lorusso, P.; Tarantino, M.; Forgione, N. Simulation of operational conditions of HX-HERO in the CIRCE facility with CFD/STH coupled codes. *Nucl. Eng. Des.* **2020**, *361*, 110552. [CrossRef]

27. Martelli, D.; Forgione, N.; Di Piazza, I.; Tarantino, M. HLM fuel pin bundle experiments in the CIRCE pool facility. *Nucl. Eng. Des.* **2015**, *292*, 76–86. [CrossRef]

28. Ambrosini, W.; Azzati, M.; Benamati, G.; Bertacci, G.; Cinotti, L.; Forgione, N.; Oriolo, F.; Scaddozzo, G.; Tarantino, M. Testing and qualification of CIRCE instrumentation based on bubble tubes. *J. Nucl. Mater.* **2004**, *335*, 293–298. [CrossRef]

29. Tarantino, M.; Martelli, D.; Del Nevo, A.; Utili, M.; Di Piazza, I.; Eboli, M.; Diamanti, D.; Tincani, A.; Miccichè, G.; Bernardi, D.; et al. Fusion technologies development at ENEA Brasimone Research Centre: Status and perspectives. *Fusion Eng. Des.* **2020**, *160*, 112008. [CrossRef]

30. Utili, M.; Bassini, S.; Boccaccini, L.V.; Bühler, L.; Cismondi, F.; Del Nevo, A.; Eboli, M.; Difonzo, F.; Hernandez, T.; Wulf, S.; et al. Status of Pb-16Li technologies for European DEMO fusion reactor. *Fusion Eng. Des.* **2019**, *146*, 2676–2681. [CrossRef]

31. Venturini, A.; Papa, F.; Utili, M.; Forgione, N. Experimental qualification of new instrumentation for lead-lithium eutectic in IELLLO facility. *Fusion Eng. Des.* **2020**, *156*, 111683. [CrossRef]

32. Narcisi, V.; Giannetti, F.; Martelli, E.; Del Nevo, A.; Tarantino, M.; Caruso, G. Steam generator mock-up preliminary design suitable for Pb-Li technology demonstration and code assessment. *Fusion Eng. Des.* **2019**, *146*, 1126–1130. [CrossRef]

33. OECD/NEA Nuclear Science Committee. *Handbook on Lead-bismuth Eutectic Alloy and Lead Properties, Materials Compatibility, Thermal Hydraulics and Technologies*; OECD: Paris, France, 2015; Available online: https://www.oecd-nea.org/jcms/pl_14972 (accessed on 22 January 2021).

34. The RELAP5 Development Team. *RELAP5 Code Manual, RELAP5/Mod3.3 Code Manual: Code Structure, System Models, and Solution Methods*; Nuclear Safety Analysis Division, Information Systems Laboratories: Idaho Falls, ID, USA, 2001; Volume 1.

35. Oriolo, F.; De Varti, A.; Fruttuoso, G.; Leonardi, M.; Bocci, S.; Forasassi, G. *Modifiche del Codice RELAP5 Versione MOD3.2 per la Simulazione di Sistemi Refrigerati con Leghe di Pb o Pb-Bi*; RL 031/00; Università di Pisa: Pisa, Italy, 2000.

36. Tarantino, M.; Del Nevo, A.; Forgione, N.; Bandini, G. Post test analysis of ICE tests. In *Volume 2: Plant Systems, Structures, and Components; Safety and Security; Next Generation Systems; Heat Exchangers and Cooling Systems, Proceedings of the 2012 20th International Conference on Nuclear Engineering, Anaheim, CA, USA, 30 July–3 August 2012*; ASME: New York, NY, USA, 2012; pp. 703–712. [CrossRef]

37. Davis, C.B. *Applicability of RELAP5-3D for Thermal-Hydraulic Analyses of a Sodium-Cooled Actinide Burner Test Reactor*; INL/EXT-06-11518; Idaho National Laboratory: Idaho Falls, ID, USA, 2006.

38. The RELAP5-3D Code Development Team. *RELAP5-3D© Code Manual Volume IV: Models and Correlations*; INEEL-EXT-98-00834; Information Systems Laboratories: Idaho Falls, ID, USA, 2006; Volume 4.

39. Rozzia, D.; Fasano, G.; Di Piazza, I.; Tarantino, M. Experimental investigation on powder conductivity for the application to double wall heat exchanger (NACIE-UP). *Nucl. Eng. Des.* **2015**, *283*, 100–113. [CrossRef]

40. Rozzia, D.; Fasano, G.; Tarantino, M.; Del Nevo, A.; Forgione, N.; Alemberti, A. Experimental investigation on powder conductivity for the application to double wall bayonet tube bundle steam generator. In Proceedings of the 24th International Conference on Nuclear Engineering for New Europe (NENE), Portoroz, Slovenia, 14–17 September 2015; pp. 214.1–214.9.

41. Shin, Y.; Gladinez, K.; Lim, J.; Marino, A.; Rosseel, K.; Aerts, A.; Van Tichelen, K. Fouling effect of lead oxide crystallization on heat transfer in LBE. In Proceedings of the 18th International Topical Meeting on Nuclear Reactor Thermal Hydraulics, NURETH 2019, Portland, OR, USA, 18–23 August 2019; pp. 1346–1359.

42. Martelli, D.; Venturini, A.; Utili, M. Literature review of lead-lithium thermophysical properties. *Fusion Eng. Des.* **2019**, *138*, 183–195. [CrossRef]